Beyond Boltzmann: thermalization of cluster catalyst ensembles can extend beyond reaction timescales

Patricia Poths,[†] Santiago Vargas,[†] Philippe Sautet,[†,‡] and Anastassia N. Alexandrova[*,†,¶]

†*Department of Chemistry and Biochemistry, University of California, Los Angeles, Los Angeles, CA 90095, USA*

‡*Department of Chemical and Biomolecular Engineering, University of California, Los Angeles, Los Angeles, California 90095, United States*

¶*California NanoSystems Institute, Los Angeles, CA, 90095, USA*

E-mail: ana@chem.ucla.edu

Abstract

The fluxionality of subnanocluster catalysts is essential for understanding their behavior at an atomistic level. Up until now, when it is at all considered, fluxionality has been treated primarily thermodynamically, representing relevant isomer populations as their Boltzmann populations. Previous work supported this, suggesting that the Pt_7/Al_2O_3 ensemble should be kinetically accessible within ns, based on the barrier heights for isomerization. In the current work, we explore the isomerization kinetics of gas-phase and surface-supported Pt_4H_x clusters, using kMC to explore the evolution of isomer populations with time as a function of temperature. We additionally revisit the previously-obtained Pt_7/Al_2O_3 network. This allows us to determine the temperature-dependent timescales at which the ensembles of these subnanoclusters reach thermal equilibirum. Gas-phase clusters readily thermalize by 350 K, while surface-supported clusters require temperatures between 500-700 K. These thermalization timescales depend on how structurally distinct the cluster isomers are within their ensemble. The greater the structural difference there is between low-energy structures, the longer it requires to reach thermal equilibrium. We show that it is essential to compute the barriers for isomerization between low-lying isomers in order to accurately determine either thermalization timescales, or non-equilibrium steady-state populations. Finally, we find that these thermalization timescales can extend to longer than catalytically-relevant timescales, depending on the reaction in question, indicating that isomerization is an essential feature of the reaction coordinate of a catalytic reaction.

TOC Graphic

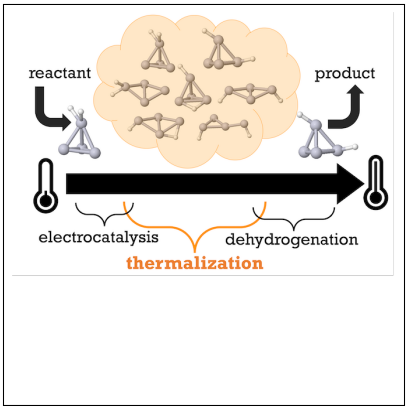

Keywords

American Chemical Society, LaTeX

Introduction

The use of metallic subnanoclusters as catalysts is highly desirable, since they display unique activity and selectivity relative to their bulk counterparts,[1–3] breaking past scaling relations that typically limit the performance of bulk catalysts.[4] Furthermore, these clusters consisting of just a few atoms on a support have a much greater atom utility than bulk, saving precious metal while operating to the same or greater effect. They can even have properties specific to their given size, such as the increased activity of Al_2O_3-supported Pt_7 clusters relative to Pt_4 and Pt_8 clusters[3] for ethylene dehydrogention, or the sinter-resistance of Pt_3 and Pt_7 clusters on TiO_2[5] or Pt_4 and Pt_7 clusters on α-Al_2O_3.[6] These subnanocluster have also been shown to be highly fluxional, meaning that they can populate and interconvert between multiple isomers at catalytically relevant temperatures,[7,8] and even dramatically change morphology within the ensemble as the partial pressure of reactants changes.[9] So far, the treatment of fluxionality has been predominantly based on the thermodynamic picture, with cluster ensembles represented by Boltzmann populations (p_i) of each isomer, calculated via the energy difference ΔE_i between the lowest-energy structure and each higher-lying one:

$$p_i = \frac{\exp -\Delta E_i / k_B T}{\sum_{j=0}^{N} \exp -\Delta E_j / k_B T} \tag{1}$$

This operates on the underlying assumption that it is possible for these clusters to reach total thermal equilibrium on timescales relevant for the chemical reaction they are catalyzing. Or in other words, that the barriers for interconversion between isomers are small compared to the barriers for reaction, and that isomerization happens much more often than the rare event of a rate-determining step.

This has been assumed to be the case, and indeed produced good qualitative agreement with experiment, for size- and composition-specific activity and selectivity in thermal catalysis, such as oxidative and non-oxidative dehydrogenation,[3,10–13] or size-dependent sinter-resistance.[6] To substantiate the assumption of the simple Boltzmann statistics, several stud-

ies were conducted. We have shown that the Al_2O_3-supported Pt_7 ensemble is broken down into two superbasins, each of which is kinetically accessible within ns, based on the heights of barriers computed between isomers in that ensemble.[14] We also showed that kinetic energy exchange upon the binding or scattering of reagents causes substantial additional cluster isomerization, helping equilibration.[15,16] However, these studies only indirectly support the Boltzmann ensemble representation. To truly capture the timescale for equilibration of an ensemble of subnanoclusters, kinetic Monte Carlo (kMC) simulations must be performed over a range of relevant temperatures, from which the final steady-state populations of each isomer could be extracted. This would reveal at what temperatures and timescales steady-state populations of isomers would be reached, and how those compare to the Boltzmann distribution. The nature of the steady state ensemble and the timescales of reaching it, when compared to the reaction rates, would provide critical mechanistic information about cluster catalysis. Recent work which has revealed the importance of this kinetic trapping explored the ability of Pt_4Ge clusters to dehydrogenate ethane selectively to ethylene.[12] As the system becomes poisoned and incorporates a C_2 unit, the active Pt_4GeC_2 isomer is expected to be over-populated relative to its Boltzmann population due to the high barrier for isomerization to the inactive state, while the corresponding Pt_4C_2 clusters can more readily access the inactive form.[13] Similarly, recent work by Peters[17] developed a simple kinetic model that treated reactivity of two different isomers as well as the fluxional conversion between them. He found that simply changing reactant concentrations and fluxionality parameters could result in dramatically different outcomes, even when equilibirum constants are kept constant. This suggests that just using the equilibrium populations of isomers is likely insufficient to predict which isomers in the ensemble contribute the most to the observed reactivity. Furthermore, recent work by Yan et al[18] investigated the populations of γ-Al_2O_3-supported $Pt_3H_{0,2}$ clusters as they underwent isomerization in conjunction with H_2 adsorption and desorption. They identified that multiple timescales are important for the restructuring of the Pt_3 cluster upon the adsorption and desorption of H_2, finding that the restructuring of Pt_3H_2 was essential for

the favorable desorption of H_2 under conditions relevant for the dehydrogenation of propane. In our work, we address the more complex system of Pt_4H_x (x=1-3), and explore the role that H coverage has on the kinetic accessibility of the entire ensemble relative to the limiting case of thermal equilibrium. It has been previously shown that increasing CO coverage on gas-phase Au_6 clusters reduces the barriers for isomer interconversion.[19] Thus we wanted to explore the role of H coverage on kinetic accessibility of Pt_4H_x cluster ensembles. We additionally revisit the Al_2O_3-supported Pt_7 system of previous work.[14] Our goal is not to identify any specific reaction channels, but to identify the temperatures and timescales at which the given ensembles reach thermal equilibrium (if the equilibrium can even be reached on the timescales of our simulations), and to reveal the influence of H coverage and the presence of a support on the process of equilibration. Pt_4H_x was chosen as a relatively simple model that still retains enough degrees of freedom to reveal the complex relationship between kinetic and thermodynamic fluxionality.

Here, we find that gas-phase clusters can typically reach thermal equilibrium at lower temperatures than surface-supported clusters, and that variable adsorbate coverage has a non-monotonic effect on ensemble kinetic accessibility. Additionally, we find that the entire Pt_7 ensemble is thermally accessible within μs at 700 K, a timescale which corresponds to the maximum barrier height for the interconversion between the two lowest energy isomers. Ultimately, even such small supported clusters as Pt_4H_3/Al_2O_3 can exhibit significant kinetic trapping resulting in non-Boltzmann steady-state populations up to 500 K. This kinetic trapping is likely highly relevant for catalytic processes that take place at temperatures below 500 K, such as electrocatalytic processes, hydrogenation, or CO oxidation. For processes such as dehydrogenation which require very high temperatures (e.g. 900 K), it is safe to assume thermal equilibration of cluster catalyst ensembles.

Methods

DFT Calculations

The gas-phase and Al_2O_3-supported Pt_4H_x ensembles were computed using in-house global optimization code, using a BLDA approach to generate starting structures that are chemically reasonable.[20] This global optimization was performed using plane-wave DFT using VASP version 5.4.4.[21] The exchange-correlation function used was PBE,[22] with PAW pseudopotentials,[23] and dDSC vdw correction,[24,25] to be consistent with previous work.[26] A plane-wave cutoff of 400 eV was used, with an energy convergence criteria of 10^{-6} eV. Geometries were considered converged when the maximum force on any atom was less than 0.02 eV $Å^{-1}$. Gas-phase clusters were placed in a 15 × 15 × 15 Åvacuum box. Surface-supported clusters were placed on a 5-layer 3 × 3 supercell of α-Al_2O_3 with a 15 Åvacuum gap as previously optimized.[3] Γ-point sampling was used for all calculations. Barriers between Pt_4H_x isomers were computed using climbing-image nudged elastic band (CI-NEB) calculations as implemented in VTST.[27,28] Isomer pairs for the identification of isomerization barriers were matched based on a rough structural similarity between either the underlying Pt core, or the arrangement of H atoms on different Pt cores. During the optimization of the CI-NEB between isomer pairs, if any local minima were found between the endpoints, a geometry optimization was performed on the intermediate structure, and full CI-NEBs were computed between each endpoint and the intermediate. If multiple intermediates were found, this was done iteratively until all local minima and saddle points were converged.

Kinetic Monte Carlo Simulation

Once all of the isomerization barriers were computed, a network connecting all of the isomers was constructed, and used as the basis for kinetic Monte Carlo (kMC) simulations. The barriers between states were converted into rates using harmonic transition state theory,

following the equation

$$k_{i \rightarrow j} = \frac{k_B T}{h} \exp \frac{-\Delta E_a}{k_B T} \tag{2}$$

where ΔE_a is the calculated energy barrier between states i and j. Within this approximation we neglect the change in vibrational entropy between the initial and transition states, which typically only changes the rate constant by a factor less than an order of magnitude.[29] The list of pairs of isomers and the barrier between them served as the representation of the network, and were fed into an in-house, rejection-free kMC code. This code was built to handle higher temperature, low barrier transitions that typically hinder KMC simulations. To achieve this, the user defines the mesh (in time) for sampling trajectory populations. As trajectories pass points along this mesh, their state is recorded, limiting the amount of memory required for simulations at higher temperatures. The user also defines the end time for their simulations and environmental temperature, which, along with the barrier matrix, completely define the kMC simulation. The implementation of pythonic classes integrates features for parallel kmc, visualization, and checkpointing. Further algorithmic tricks were used to leverage C-interfaced packages in python such as batched random number generation, checkpointing, and numba/jit. This code is freely-available at https://github.com/santi921/kmcluster.

In order to evaluate the evolution of isomer populations with time, 10,000 kMC trajectories for each network at a given temperature were launched, each one starting from a randomly-selected isomer. This random initial population of isomers may represent the case where atomically-precise subnano clusters are deposited on a support in a kinetically trapped state. The 10,000 kMC trajectories were run until all trajectories reached 0.0001 s, or 100 μs. The isomer populations were sampled every 0.1 μs along the trajectories for visualization and population analysis.

The temperature ranges used varied somewhat for each system composition, as each one has a different range of low energy barriers which limit the advance of the kMC clock with each step- a common problem in kMC.[30] For the gas-phase clusters, kMC simulations between 100 and 450 K were performed, enough to explore the thermalization of the full networks. For the

surface-supported clusters, the simulations could also generally be performed up to 450 K, however this was not enough to identify the temperature/timescales at which the networks reach thermal equilibrium. In order to reach higher temperatures, the surface-supported networks were coarsened to (a) only the most relevant pathways and (b) to barriers between states that were ≥ 0.2 eV in both directions, collapsing any states with a low barrier between them into a single state represented by the lowest energy of the multiple states.

Once the kMC trajectories were complete, isomer populations were assessed as a function of time. The final isomer populations were compared with the Boltzmann populations of the ensemble at the corresponding temperature. Additionally, the time taken for the cluster to reach a steady-state was assessed.

Results and discussion

Gas-Phase Clusters

We first explore the isomerization of gas-phase Pt_4H_x x=1-3 clusters, and study the effect of hydrogen coverage on cluster isomerization. Varying coverages can be accessed by Pt clusters under different reaction conditions, and as a function of the stage of the catalyzed reaction. The adsorbate coverage is known to cause changes in ensembles and relative energetic ordering of the isomers.[9,19] The global optimization and of Pt_4H_x (x = 1-3) gas-phase clusters was performed, followed by CI-NEBs to determine isomerization barriers. The networks connecting all isomers are shown in Figure 1 (a)-(c). The ensembles of structures for each network are shown in Figures S1-S3.

These networks provide useful general chemical information: For instance, somewhat surprisingly, the barriers for H migration on the Pt_4 core are not significantly smaller than the barriers involving restructuring of the Pt_4 core. This means that when considering reactivity involving adsorbate migration, cluster isomerization can be an important aspect of the reaction coordinate, as was recently shown for Pt_3H_2.[18] However, for Pt_4H_x, we find much

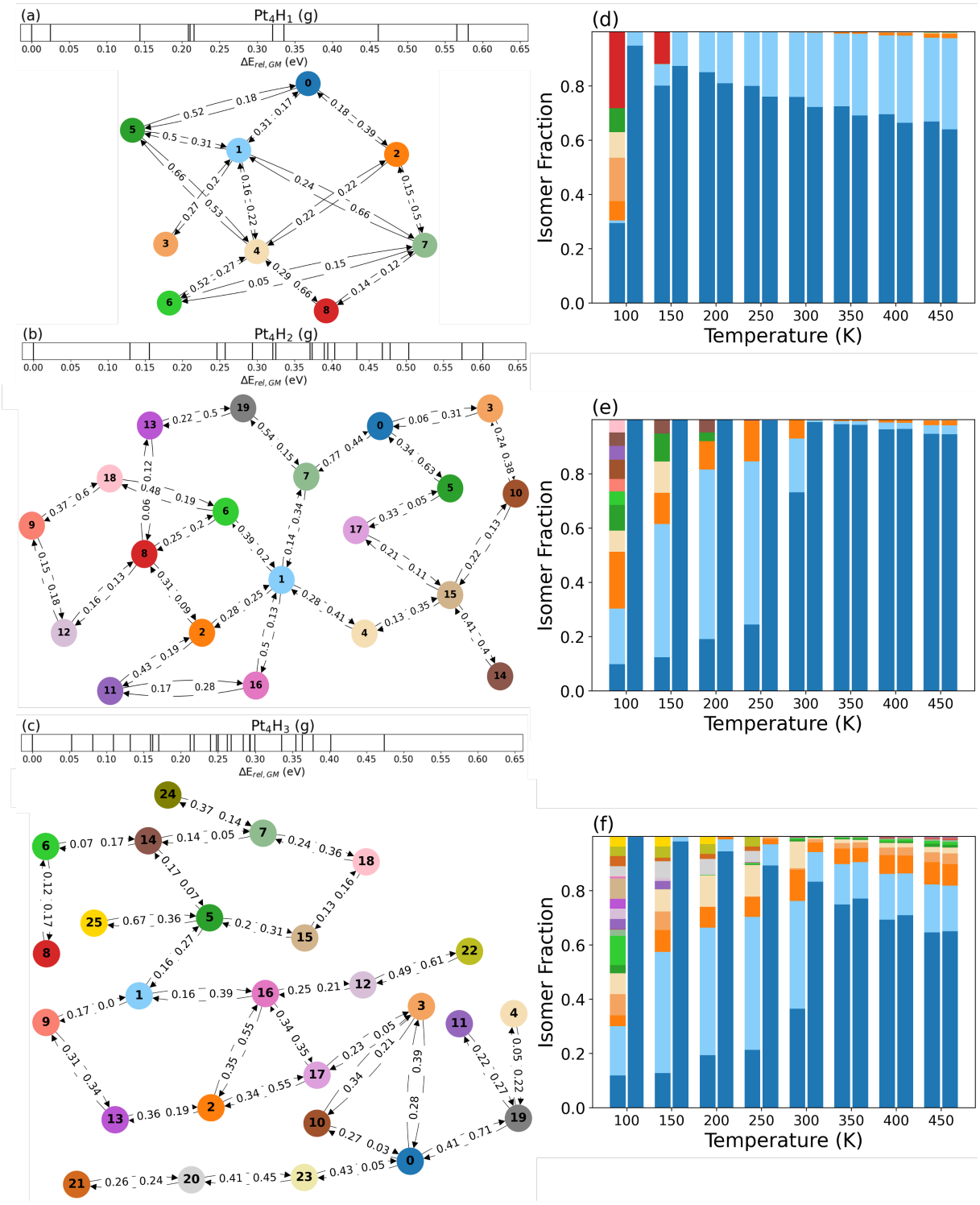

Figure 1: Isomerization networks for gas-phase (a) Pt_4H_1, (b) Pt_4H_2, and (c) Pt_4H_3, with isomer relative energies shown above. Each node is an isomer, labeled in the order of increasing energy (starting index 0). Edge labels represent barriers between isomers, direction indicated by value closest to arrow heads. Isomer distributions for each composition from 100 - 450 K after 10^{-4} s are shown in (d) - (f); the left-hand bar displays the isomer population at the end of each kMC simulation (100 μs), while the right-hand bar displays the Boltzmann populations at each temperature. Node colors in (a)-(c) map to isomer colors in (d)-(f).

less separation of H migration and Pt restructuring. kMC sampling is performed on the shown networks, in order to explore the time evolution of isomer populations across a range of temperatures. The evolution of the relative populations of each isomer over the 100 μs simulations are then plotted for each temperature, to show how isomer populations change with time (see Figure S4 - S6). The final isomer populations of each of these simulations at each simulated temperature are plotted in Figure 1 (d) - (f), and compared to the corresponding Boltzmann populations of the isomers.

It is immediately clear that Pt_4H_1 reaches the thermal equilibrium at the end of the kMC simulation by 200 K. Looking at the time-resolved isomer populations, however, we see that this takes up to 2 μs. By 250 K, however, it takes ca. 50 ns. In contrast, Pt_4H_2 and Pt_4H_3 require higher temperatures to reach thermal equilibrium within the timeframe of the simulations. For Pt_4H_2 it takes 25-30 μs at 350 K, and ca. 2 μs at 400 K. For Pt_4H_3 it takes 80 μs at 350 K, and 5 μs at 400 K. Clearly, as the hydrogen coverage of the gas-phase Pt_4 clusters increases, the thermal equilibration is slowed down.

The differences in the networks show in Figure 1 (a) - (c) hold an explanation for the observed behavior. Pt_4H_1 has a fairly simple and closely-connected network; many isomers are accessible from multiple other isomers, and the global minimum (GM) isomer (index 0 in network) and next-lowest isomer (index 1) are directly connected. This is because they are structurally quite similar (see Figure S1), and do not pass through an intermediate structure upon isomerization. Converting between most isomers does not require multiple steps with significant geometric rearrangement. Almost every isomer can be reached from every other isomer via one intermediate. The same cannot be said for Pt_4H_2 and Pt_4H_3.

For the Pt_4H_2 network in Figure 1(b), we see that the pathways to reach other isomers can be quite long, with multiple intermediate states. Furthermore, the two lowest energy isomers, 0 and 1, are separated by the isomer 7, with a barrier of 0.77 eV for isomer 0 to reach isomer 7. (Figure 2(a)) The reason for this is structural: (see Figure 2(a)). While isomers 0 and 1 have a similar Pt_4 core, the migration of H between the atop sites must go through an

intermediate with a bridging H. Within the Pt_4H_2 ensemble, isomers with bridging H atoms

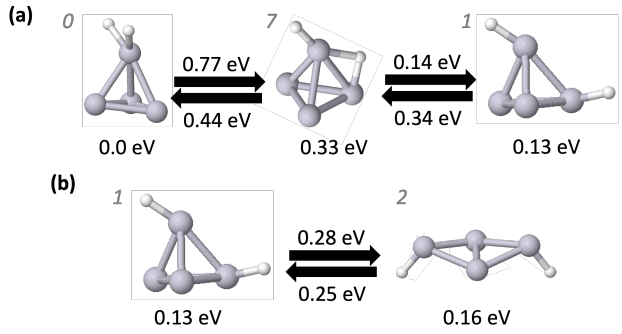

Figure 2: Representative isomerization pathways between gas-phase Pt_4H_2 isomers, with typically low and high barriers. The shown isomer energies are relative to isomer 0. Barriers are given relative to the starting structure.

are generally higher in energy than those with only atop H atom coordination. Thus, any H migration between Pt atoms will inevitably go through a high-energy intermediate, crossing a high barrier. In contrast, in the isomerization between isomers 1 and 2, breaking the Pt-Pt bond has a low barrier, of only 0.28 eV (Figure 2 (b)). However, to access 2 from 0 still requires that the system passes through isomer 7. Additionally, just by visual inspection, the ensemble of structures for Pt_4H_2 features a much greater structural diversity than that for Pt_4H_1 (Figure S1 vs. S2). The low-lying isomers are therefore separated by much higher energy intermediate structures, creating kinetic hindrances for the thermalization. Even the addition of just a second H atom can cause a slowdown of ensemble thermalization.

The behavior of Pt_4H_3 is even more extreme than Pt_4H_2, with isomers 0 and 1 separated by 5 intermediates, and a network structure that is much more branching than Pt_4H_1 and Pt_4H_2. This is because having 3 H adds a significant number of degrees of freedom, in particular allowing for more H arrangements on each possible Pt_4 core structure. The variety in the Pt_4 core structures is also greater at this coverage. The structural diversification and network complexity lead to slower thermal equilibration compared to Pt_4H_1 and Pt_4H_2, as reflected in Figure 1(f). This is despite the fact that, based on Boltzmann populations, the ensemble is more thermally accessible, as reflected in the higher Boltzmann populations of metastable isomers shown in in Figure 1(f). This arises from metastable isomers being closer in energy

to the GM isomer, as reflected in the plot of isomer energies in Figure 1(c). However, as these structures which are similar in energy are structurally very different, we get kinetic trapping.

Here we have found that, for gas phase clusters, increasing H coverage results in longer thermalization times (or higher temperatures). This is due to the fact that that adding H causes more significant structural differences between low-lying isomers, and that results in higher barriers to isomerization between them. Essentially, increasing the number of adsorbates results in a more jagged, difficult to traverse PES. Next, we examine the added effect of the support.

Surface-Supported Clusters

Pt_7/Al_2O_3

The full isomerization network for Pt_7 on α-Al_2O_3 was previously published.[14] The Pt_7/Al_2O_3 structures can be seen in Figure S7. In order to access reasonable temperatures and timescales with kMC, a small amount of coarsening was done to yield the isomer energy distribution and network shown in Figure 3 (a) and (b), respectively. This coarsening consisted of combining structurally similar states that were separated by barriers less than 0.1 eV into a single state. These states are highlighted in Figure S8. We were able to perform kMC simulations up to 400 K with this network, the final isomer distributions of which are compared to the corresponding Boltzmann populations in Figure 3 (c). Much like for gas-phase clusters, lower temperatures result in many isomers remaining present in kinetically-trapped states, while at higher temperatures the system relaxes to populations of just a few key isomers. However, this Pt_7 network does not thermalize within accessible simulation temperatures. Even by 400 K, the system is stuck with a population of isomer 1 that is dramatically higher than its equilibrium population. (0.65 vs 0.11). For temperatures between 200 and 350 K, some isomer populations are still evolving at the end of the 100 μs run, albeit very slowly (Figures 3 (d), S9). In contrast, at 400 K we see that the populations of isomers 0 and

1 are essentially flat, indicating that the system has reached a quasi-steady state, with an artificially high population of isomer 1. While this line looks very flat, we can fit the linear

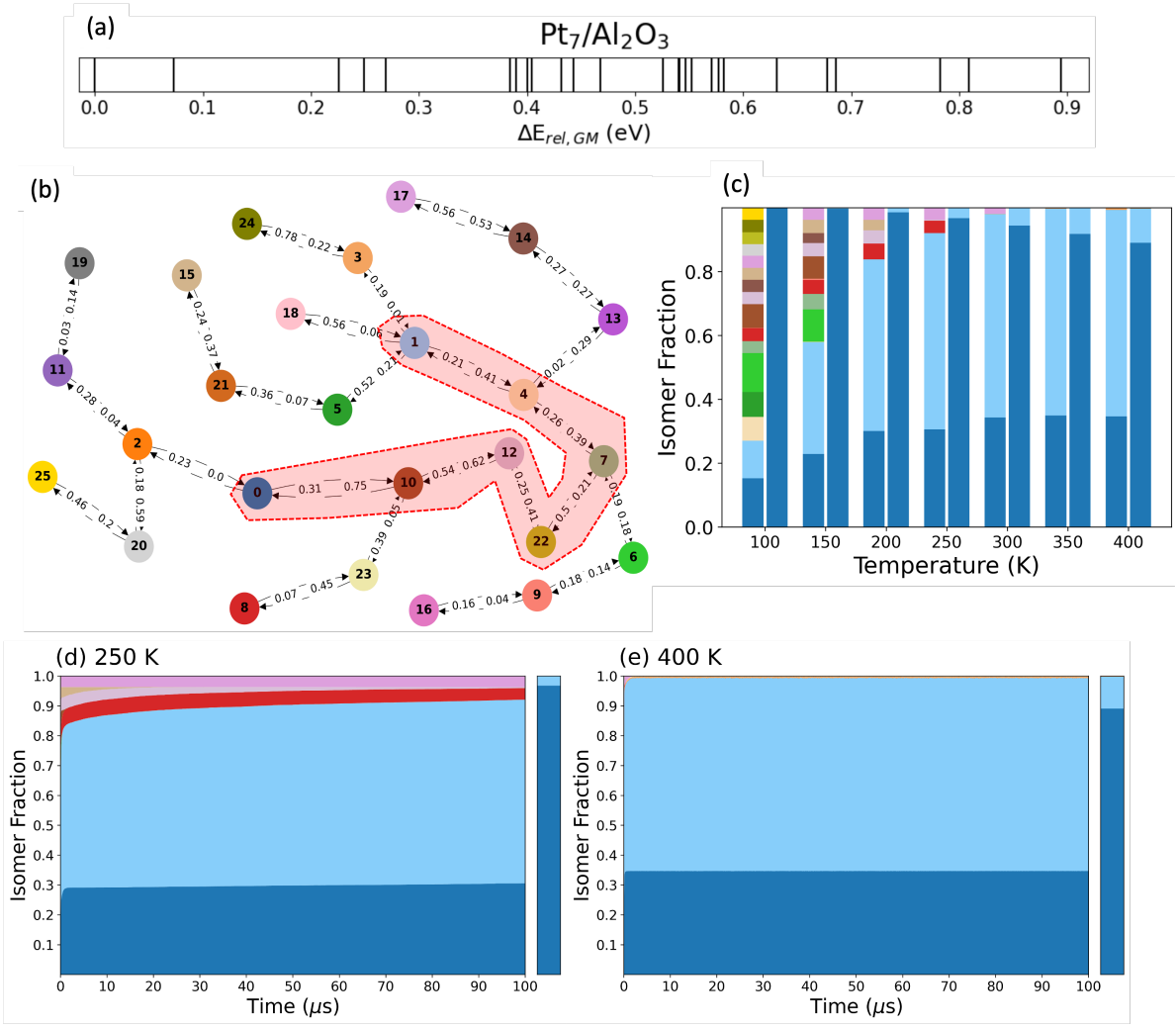

Figure 3: Pt_7/Al_2O_3 isomer energy distribution (a) and isomerization network (b) taken from[14] and slightly coarsened to run with kMC. (c) Comparison of the full network kMC simulations with time (left bars) with the Boltzmann populations at the corresponding temperatures (right). (d) and (e) show stacked plots of isomer populations for 250 K and 400 K respectively, highlightng a kinetically-trapped system, and one that is thermalizing, but on timescales longer than 100 μs. The color representing isomers in (c) - (e) matches the labels in the network in (b).

portion of the line and extrapolate to the point at which the population of isomer 1 would reach 0.89, which is its corresponding Boltzmann population at 400 K, as can be seen in Figure 3 (c). This yields a time of 0.53 s, which is many orders of magnitude longer than we

could simulate with kMC. This is only a rough estimate of the lower limit of the time taken to reach the Boltzmann population of the GM only, as growth of the GM population should not stay linear, but rather should turn asymptotic over time. We note in passing that the timescales at which different isomers relax to a steady state at the same temperature differ. (Figure S9).

Running kMC on the Pt_7/Al_2O_3 network in Figure 3 (b) does not allow us to directly determine the timescales required at any temperature to reach thermal equilibrium. To access this information, we instead use a sub-network that captures the important information about the superbasins around minima 0 and 1, as these are the two isomers with significant populations at the end of the kMC simulations. This was previously determined through analysis which separated the network down into two superbasins.[14] To do this, we reduce the network from Figure 3 to just the chain of states connecting isomers 0 and 1. This sub-network is highlighted on the network displayed in Figure 3(b). The isolated chain of states is shown in Figure 4 (a).

We performed kMC simulations on this chain of states from 300 K to 700 K in order to ensure that the low-temperature behavior of the full network was suitably approximated. The relative populations of 0 and 1 of the sub-network are similar to that of the full network at 300 K and 400 K, allowing us to trust the behavior at higher temperatures. Ultimately, we are most interested in when isomers 0 and 1 reach thermal equilibrium with each other. Isomer 1 was previously shown to be more catalytically relevant than 0 for ethylene dehydrogenation,[3] so understanding the conversion between them is relevant. We note that, for both the full and minimal chain Pt_7/Al_2O_3 networks, we see a significant over-population of isomer 1 in kinetically trapped states compared to the corresponding Boltzmann populations. This is because more of the ensemble structures are within the superbasin around isomer 1,[14] and thus relax preferentially to population isomer 1 instead of isomer 0.

For the minimal system, we see that at 600 K the system thermalizes within ca. 60 μs. At 700 K, the time to thermalize becomes on the order of ca. 5 μs. If we compare this

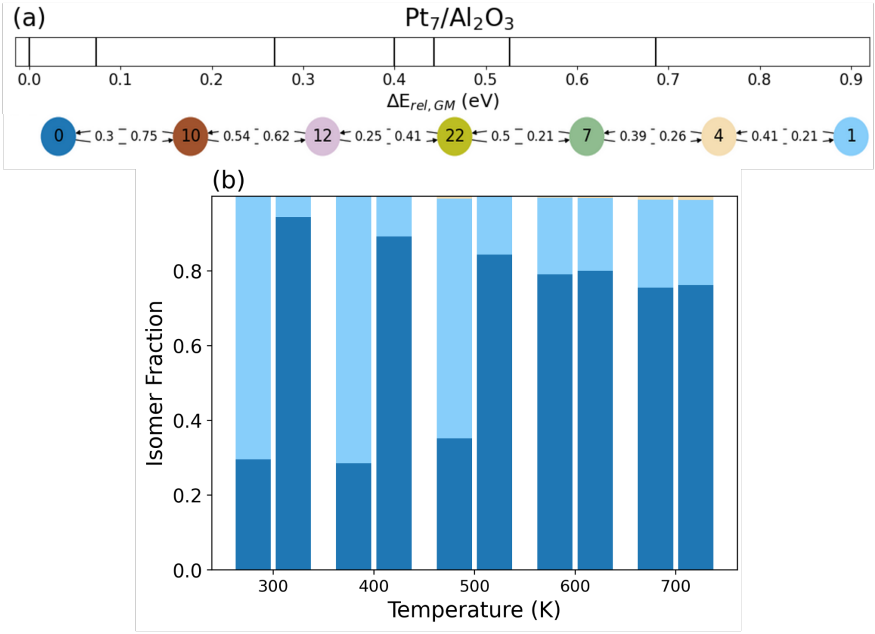

Figure 4: (a) Relative energies of the most revenant isomers and the path connecting only Pt_7 isomers 0 and 1. (b) Isomer distributions at the end of the 100 μs kMC simulation (left bar) and their corresponding Boltzmann populations (right bar) for each temperature. Note that much higher temperatures an be accessed with this simpler approach, showing that the Pt_7 system has reached thermal equilibrium within μs by 600 K.

to the estimated rate of passing a 0.936 eV barrier, which is the effective maximum barrier between isomers 0 and 1, we find a rate of 2.66 $\times 10^6$ Hz, or a timescale of ca. 3.8 $\times 10^{-7}$. This is within one order of magnitude of the estimated timescale given by the kMC simulation. Therefore, one can get a decent estimate of the timescale for the equilibration of a system dominated by two superbasins by identifying the maximum barrier between the minima of each basin. Likely this could be extended to systems with more than two basins by considering the maximum barriers between the basins. T

Pt_4H_x/Al_2O_3

Next, we study the Al_2O_3- supported Pt_4H_x clusters, and explore the interaction between adsorbate coverage and binding to a support on the kinetic accessibility of ensembles. For the surface-supported Pt_4H_x clusters, we again perform a global optimization for each composition, match up the isomers in a pairwise fashion, and compute the barriers for isomerization

using CI-NEB. The resultant networks are shown in Figure 5 (a) - (c). The corresponding ensembles of structures are shown in Figures S11-S13.

For H-covered Pt_4 clusters, the presence of the α-Al_2O_3 surface results in a dramatic increase in time or temperature required for thermalization, compared to the corresponding gas-phase clusters. This makes sense; the clusters are interacting strongly with the support, suppressing isomerization, as more bonds must be broken than in the gas phase. A one-to-one comparison of the cluster isomerization in the gas phase and on the support is difficult, because the presence of the support changes the accessible ensembles of clusters. However, for the isomerization processes involving similar Pt and H motions, the barriers are significantly higher when the clusters are supported versus in the gas phase.

We analyze the thermalization rate of supported clusters as a function of H coverage (Figure 5 (d)-(f)). Pt_4H_2/Al_2O_3 reaches thermal equilibrium at 550 K (the highest temperature that could be reached with any full network) within ca. 40 μs. However, neither Pt_4H_1/Al_2O_3 nor Pt_4H_3/Al_2O_3 even approach thermal equilibrium within 100 μs at 450 K (the highest temperature accessible via kMC on the full networks, in these cases). See Figures S14 and S15 for the time evolution. The difference in thermalization ability as a function of H coverage is due to differing structures of the networks seen in Figure 5 (a) - (c). For Pt_4H_2 (Fig. 5b), most isomers are connected to multiple others, leading to a strongly inter-connected network. $Pt_4H_1Al_2O_3$ and $Pt_4H_3Al_2O_3$, on the other hand, have networks with long chains and significant branching. Thus, some isomerization paths are very long, passing through many intermediate structures, reducing the chance of moving forward with isomerization, rather than backward. Furthermore, the full Pt_4H_2/Al_2O_3 ensemble has fewer high energy intermediate structures overall, compared to Pt_4H_1/Al_2O_3 and Pt_4H_3/Al_2O_3 - see isomer energy distributions in Figure 5 (a) - (c). Thus it does not have as many high-energy isomers separating lower-energy isomers. This results in a flatter potential energy surface of Pt_4H_2/Al_2O_3 that is easier to traverse.

For Pt_4H_1/Al_2O_3 and Pt_4H_3/Al_2O_3, the low-lying isomers are more structurally distinct from

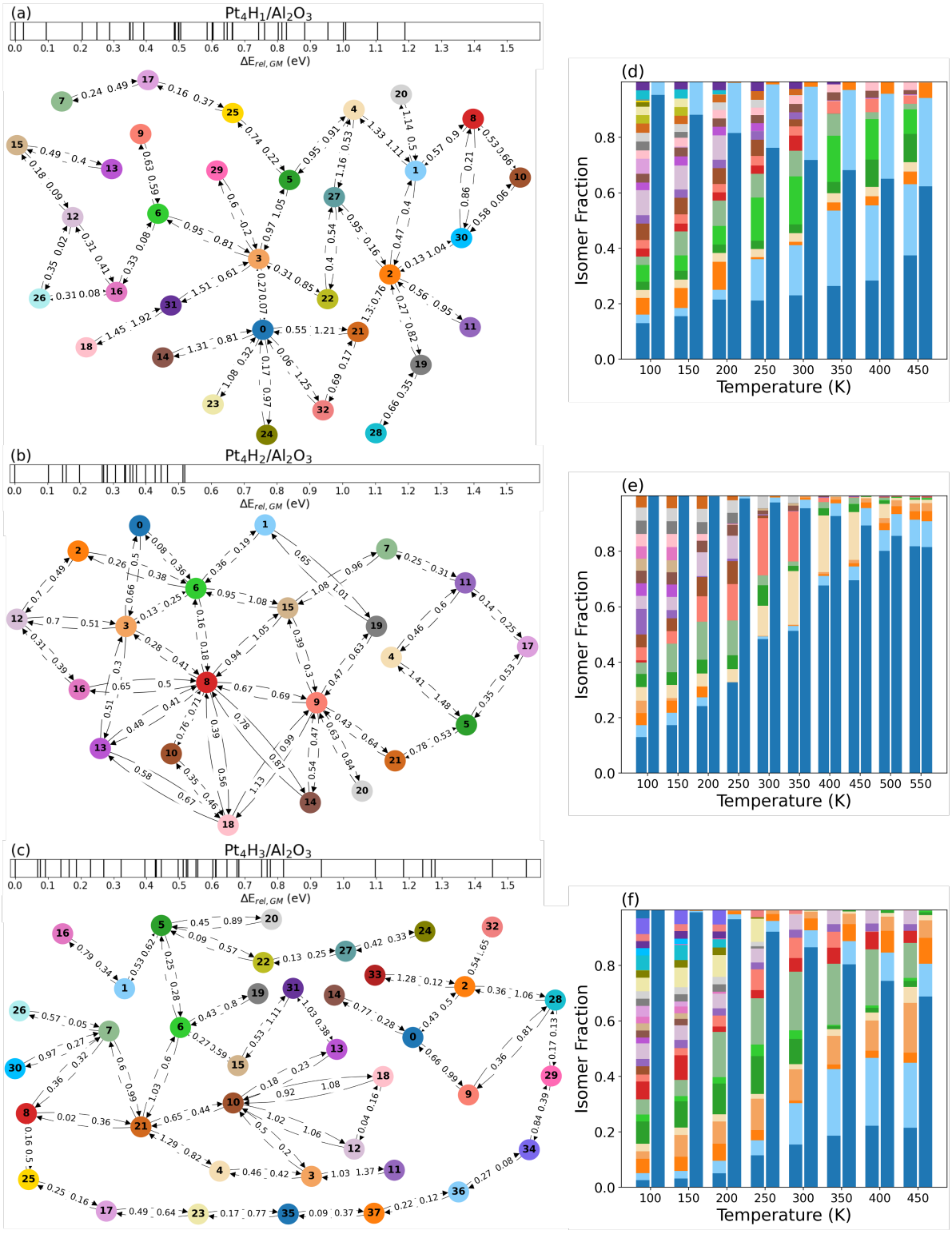

Figure 5: (a)-(c) Networks for Pt_4H_{1-3} on α-Al_2O_3. (c) - (d) isomer distribution plots comparing distributions at the end of the kMC simulation (left) and Boltzmann populations (right) at each given temperature.

each other, and must pass through multiple higher-lying structures during thermalization. (See Figures S11, S13) In other words, the low-lying $Pt_4H_{1,3}/Al_2O_3$ isomer structures are more "separate" from each other on their respective PESs than is the case for Pt_4H_2/Al_2O_3. Interestingly, this degree of "separation" of the most stable local minima is not a function of how many isomers are thermally accessible based solely on their energy differences. Pt_4H_3/Al_2O_3 has many more "thermally accessible" isomers than Pt_4H_2/Al_2O_3, as can be seen by the Boltzmann distribution of isomers in Figure 5 (b) and (c). By 450 K, isomers 0 through 5 gain significant enough populations during a kMC trajectory, with isomer 0 only consisting of 0.65 of the entire ensemble. Pt_4H_1/Al_2O_3 is similar- the GM takes up only 0.60 of the entire ensemble at 450 K. However, much of the rest of the ensemble is populated by isomer 1, with a fraction of isomer 2. Thus, while the GM represents a smaller fraction of the ensemble, the entire Pt_4H_1/Al_2O_3 ensemble has less diversity in thermally accessible isomers. Pt_4H_2/Al_2O_3, in contrast, is mostly dominated by the GM, indicating that less of the ensemble is thermally accessible. This is despite the fact that its ensemble is more kinetically accessible than the other two H coverages. Hence here we see the paradox between thermal accessibility and kinetic accessibility for fluxional subnanoclusters. The more "thermally accessible" an ensemble is, with more distinct low-energy isomers, the less kinetically accessible it becomes, due to the significant rearrangement required to isomerize between the low-lying states.

An attempt was made to produce minimal networks for Pt_4H_x/Al_2O_3, in order to access simulations with higher temperatures to try and reach thermal equilibrium. We focused only on the isomers that dominated the kinetically trapped ensembles in Figure 5, producing the networks in Figure S17 (a) - (c). The comparisons between kMC populations and Boltzmann populations can be seen in the Figure S17 (d) -(f). Despite detailed balance being maintained, the populations fail to equilibrate to the Boltzmann statistics within the simulation timescale. Pt_4H_1/Al_2O_3 reaches an isomer 0 population at the end of the kMC simulation that is higher than the equivalent isomer 0 Boltzmann population. For Pt_4H_2,

at high temperatures, isomer 8 population in the kMC simulations is higher than its corresponding Boltzmann population. The network for Pt_4H_3/Al_2O_3, in contrast, is similar to that of Pt_7/Al_2O_3, where two structurally distinct low-lying isomers are separated by a long path consisting of many intermediates. And much like Pt_7, the Pt_4H_3/Al_2O_3 network shows kinetic trapping even up to 750 K (Figure S17).

The observed differences in isomerization kinetics, including the dramatic isomerization slowdown, are governed by the structural diversity within the ensembles, due to two distinct but interdependent degrees of freedom: the structure of the Pt_4 core, and the placement of the H atoms on this core. Increased H coverage tends to open up the Pt core and diversify the accessible geometries.[9] This adsorption-driven diversification of the core structures appears to lead to greater kinetic trapping, compared to ensembles with minimal structural diversity, as it results in many lengthy, multi-step isomerization pathways between low-lying intermediates. A possible limitation of this work is incomplete sampling, despite the effort to make it as exhaustive as possible. However, we can draw several general conclusions. For both gas-phase and surface-supported clusters of varying compositions, trapping follows the "distance" between the lowest local minima on the PES, as measured by the number of intermediates along isomerization paths, or by significant structural differences. This effect depends on the structural ensemble of clusters.

Thermalization versus Reaction Timescales

In order to place the thermalization timescales in comparison to timescales of typical catalyzed reactions, we estimated the effective barriers for reactions with TOF of ca. 1 s^{-1} at a range of temperatures. These estimations are summarized in Table 1. We then compare these barriers to (a) the maximum barriers between low-lying intermediates for each system, and (b) to the effective barriers for the systems where we directly observe the thermalization timescale (Table 2). It is immediately obvious that, for the gas phase clusters which have smaller networks, the approximated barrier based on the thermalization timescale matches

Table 1: Effective barriers that must be overcome for catalytic reactions from 300 - 900 K with a TOF of 1 s^{-1}, to compare with the barriers for thermalization of Pt_4Hx and Pt_7.

Temperature (K)	Effective E_a (eV)
300	0.52
400	0.71
500	0.89
600	1.08
700	1.27
800	1.46
900	1.66

well the maximum barrier between low-lying intermediates. The one exception is Pt_4H_1, though this is because we take the highest barrier leaving state 0. The effective barrier for

Table 2: Comparison between the maximum barrier extracted from the isomerization network, and the effective barrier for thermalization extracted from kMC simulation outputs.

Cluster	Max. Barrier (eV)	Effective Barrier (eV)	Thermalization (K)
Pt_4H_1	$0 \rightarrow 2 = 0.39$	0.29	$<< 300$
Pt_4H_2	$0 \rightarrow 1 = 0.64$	0.58	300-350
Pt_4H_3	$0 \rightarrow 1 = 0.64$	0.60	350
Pt_7/Al_2O_3	$0 \rightarrow 1 = 0.94$	1.07	600
Pt_4H_1/Al_2O_3	$0 \rightarrow 1 = 1.19$	0.85-0.95	450-500
Pt_4H_2/Al_2O_3	$0 \rightarrow 4 = 1.37$	0.946	550
Pt_4H_3/Al_2O_3	$0 \rightarrow 1 = 1.67$	1.12-1.22	600-650

thermalization is lower, because the network does not have distinct basins, and with a random distribution of initial isomer states, the heights of the barriers going from a high energy state to a lower one are also important. For Pt_7/Al_2O_3, we also see that the estimated effective barrier based on thermalization timescale is quite close to the actual maximum barrier between isomers 0 and 1.

For the surface-supported Pt_4H_x clusters, however, the situaiton is different. Only for Pt_4H_2/Al_2O_3 can we directly access the thermalization timescales with our kMC simulations. For Pt_4H_1/Al_2O_3 and Pt_4H_3/Al_2O_3, we estimate the timescale for thermalization based on the extrapolation of a linear fit of the isomer 0 population to its Boltzmann population.

We note that this is likely a crude lower bound for the effective barrier. To estimate the extent to which this is a crude lower bound, we did the same kind of linear fit for the 500 K Pt_4H_2/Al_2O_3 simulation, doing a linear fit between 5 μs and 25 μs. This yielded an effective barrier of 0.88 eV, compared to the effective barrier of 0.946 eV extracted from the 550 K fit. Thus we estimate that the barriers for $Pt_4H_{1,3}/Al_2O_3$ should be at least 0.1 eV higher. We do note, however, that the relative effective barriers with increasing H coverage match roughly relative increase of the maximum barriers extracted for each cluster composition. This suggests that for the H-decorated Pt_4 clusters, the maximum barrier between low-lying states is alone not enough to estimate the timescale for equilibration.

Taking the effective barriers for thermalization, we compare them to the effective barriers for catalytic processes with a TOF of 1 s^{-1} in Table 1. From the comparison, we estimate the temperatures at which the clusters would reach thermal equilibrium on the same timescales as a reaction at a given temperature. We note the difference between the thermalization we observed in kMC (within 100 μs), and within the timescale relavant for catalysis (relative to a TOF of 1 s^{-1}). The gas-phase clusters thermalize within the trajectory timeframe by 300-400K, and therefore treating them as thermally equilibrated for any process that runs at room temperature and above, such as any electrochemical process, would be an accurate approximation. However, surface-supported clusters tend to reach thermal equilibrium within the temperature range of 500-650 K during the trajectory. This means that in electrochemical processes, which take place at room temperature, the ensemble of cluster catalysts would not be fully-equilibrated. Processes such as hydrogenation or CO oxidation, which occur at temperatures from 400-550 K are borderline cases, where the full equilibration of the system might not take place. Equilibration within superbasins is more likely. For very high-temperature processes, such as dehydrogenation, which take place at 900 K, it is safe to assume that the cluster ensembles are fully thermalized.

Conclusion

In the past, Boltzmann statistics have been assumed to be sufficient to describe the fluxional nature of metallic subnanocluster catalysts. This approach, over the treatment of a single stable structure, has yielded results in better agreement with experiment for aspects such as cluster size- and composition-dependent activity, selectivity, and interpretation of spectra.[3,6,10–13,31,32] Barrier heights for the isomerization of the Pt_7/Al_2O_3 ensemble suggested that sub-ensembles should be fully accessible within ns.[14] However, this approach has always assumed that the entire ensemble of structures reaches thermal equilibrium between each step of the catalytic reaction. This would require the barriers for cluster isomerization in the presence of adsorbates to be lower than the barriers for each elementary reaction step. In order to assess the validity of this assumption, we developed a kMC protocol to evaluate the thermalization timescales at variable temperatures. Pt clusters are shown to exhibit thermalization timescales that are support-, coverage-, and size-dependent. Some clusters exhibit significant kinetic trapping even up to 700 K. The degree of kinetic trapping depends on the nature of the isomerization network of a given cluster composition. Ensembles where low-lying isomers exhibit large structural diversity are more likely to become kinetically trapped, as significant rearrangement through multiple high-energy intermediates is required to convert between them. This kind of diversity in cluster structure is promoted by reactant adsorption, as previously shown for Pt_8 clusters,[9] Pt_4 and Pt_4Ge clusters,[12,13] as well as observed in the current work. Based on the temperatures at which our ensembles thermalize, we predict that thermal equilibration of cluster ensembles on the timescales faster that the rection TOF, occurs for processes that require very high temperatures, such as dehydrogenation. In contrast, room-temperature processes such as electrocatalysis likely experience significant kinetic trapping of ensembles. Catalytic processes that operate under moderate conditions, such as hydrogenation or CO oxidation, are borderline cases, where the precise operation conditions of experiment are required to determine if the cluster ensemble can be treated as thermalized on the timescales faster than the reaction TOF.

Consideration of specific, kinetically-driven cluster ensemble thermalization as part of the catalytic reaction coordinate is therefore clearly important, for the accurate identification of active sites and realistic reaction mechanisms. We note that small clusters are among the most fluxional catalytic systems, with arguably the greatest structural diversity. More bulk-like fluxional catalytic interfaces, such as dynamic amorphous films or surfaces of larger nanoparticles, may in fact exhibit less kinetic trapping because the structural diversity in their ensembles may be strongly restricted by the bulk structure beneath. This would mean shorter isomerisation pathways and faster thermalization. On the other hand, if the bulk structure imposes higher isomerization barriers, thermalization can be slowed down. Thermalization of such interfaces will be subject of future studies.

Acknowledgement

This work was supported by the grant DE-SC0019152 from the U.S. Department of Energy, Office of Science, Basic Energy Science Program. Computational resources were provided by the National Energy Research Scientific Computing Center (NERSC), a U.S. Department of Energy Office of Science User Facility operated under Contract DEAC02- 05CH11231, and Theta of the Innovative and Novel Computational Impact on Theory and Experiment (INCITE) program at the Argonne Leadership Computing Facility, a U.S. Department of Energy Office of Science User Facility operated under Contract DE-AC02-06CH11357. S.V. would also like to thank the U.S. Department of Energy, Office of Science, Office of Advanced Scientific Computing Research, Department of Energy Computational Science Graduate Fellowship under Award Number DE-SC0020347.

Supporting Information Available

Ensembles of structures for gas-phase and Al_2O_3-supported Pt_4H_x clusters. Plots of isomer population with time over a range of temperature during kMC simulations. Coarsened

networks and isomer distribution plots for Pt_4H_x/Al_2O_3.

References

(1) Vajda, S.; Pellin, M. J.; Greeley, J. P.; Marshall, C. L.; Curtiss, L. A.; Ballentine, G. A.; Elam, J. W.; Catillon-Mucherie, S.; Redfern, P. C.; Mehmood, F. et al. Subnanometre platinum clusters as highly active and selective catalysts for the oxidative dehydrogenation of propane. *Nature Materials* **2009**, *8*, 213–216.

(2) Kaden, W. E.; Wu, T.; Kunkel, W. A.; Anderson, S. L. Electronic Structure Controls Reactivity of Size-Selected Pd Clusters Adsorbed on TiO_2 Surfaces. *Science* **2009**, *326*, 826–829.

(3) Baxter, E. T.; Ha, M.-A.; Cass, A. C.; Alexandrova, A. N.; Anderson, S. L. Ethylene Dehydrogenation on $Pt_{4,7,8}$ Clusters on Al_2O_3: Strong Cluster Size Dependence Linked to Preferred Catalyst Morphologies. *ACS Catalysis* **2017**, *7*, 3322–3335.

(4) Zandkarimi, B.; Alexandrova, A. N. Dynamics of Subnanometer Pt Clusters Can Break the Scaling Relationships in Catalysis. *The Journal of Physical Chemistry Letters* **2019**, *10*, 460–467.

(5) Zandkarimi, B.; Poths, P.; Alexandrova, A. N. When Fluxionality Beats Size Selection: Acceleration of Ostwald Ripening of Sub-Nano Clusters. *Angewandte Chemie* **2021**, *133*, 12080–12089.

(6) Poths, P.; Hong, Z.; Li, G.; Anderson, S. L.; Alexandrova, A. N. "Magic" Sinter-Resistant Cluster Sizes of Pt_n Supported on Alumina. *The Journal of Physical Chemistry Letters* **2022**, *13*, 11044–11050.

(7) Zandkarimi, B.; Alexandrova, A. N. Surface-supported cluster catalysis: Ensembles of metastable states run the show. *WIREs Computational Molecular Science* **2019**, *9*.

(8) Zhang, Z.; Zandkarimi, B.; Alexandrova, A. N. Ensembles of Metastable States Govern Heterogeneous Catalysis on Dynamic Interfaces. *Accounts of Chemical Research* **2020**, *53*, 447–458.

(9) Sun, G.; Alexandrova, A. N.; Sautet, P. Pt_8 cluster on alumina under a pressure of hydrogen: Support-dependent reconstruction from first-principles global optimization. *The Journal of Chemical Physics* **2019**, *151*.

(10) Halder, A.; Ha, M.-A.; Zhai, H.; Yang, B.; Pellin, M. J.; Seifert, S.; Alexandrova, A. N.; Vajda, S. Oxidative Dehydrogenation of Cyclohexane by Cu ivs/i Pd Clusters: Selectivity Control by Specific Cluster Dynamics. *ChemCatChem* **2020**, *12*, 1307–1315.

(11) Gorey, T. J.; Zandkarimi, B.; Li, G.; Baxter, E. T.; Alexandrova, A. N.; Anderson, S. L. Coking-Resistant Sub-Nano Dehydrogenation Catalysts: Pt_nSn_x/SiO_2 (n = 4, 7). *ACS Catalysis* **2020**, *10*, 4543–4558.

(12) Poths, P.; Li, G.; Masubuchi, T.; Morgan, H. W. T.; Zhang, Z.; Alexandrova, A. N.; Anderson, S. L. Got Coke? Self-Limiting Poisoning Makes an Ultra Stable and Selective Sub-Nano Cluster Catalyst. *ACS Catalysis* **2023**, *13*, 1533–1544.

(13) Poths, P.; Morgan, H. W. T.; Li, G.; Fuchs, A.; Anderson, S. L.; Alexandrova, A. N. Promoter–Poison Partnership Protects Platinum Performance in Coked Cluster Catalysts. *The Journal of Physical Chemistry C* **2023**, *127*, 5376–5384.

(14) Zhai, H.; Alexandrova, A. N. Local Fluxionality of Surface-Deposited Cluster Catalysts: The Case of Pt_7 on Al_2O_3. *The Journal of Physical Chemistry Letters* **2018**, *9*, 1696–1702.

(15) Guo, H.; Sautet, P.; Alexandrova, A. N. Reagent-Triggered Isomerization of Fluxional Cluster Catalyst via Dynamic Coupling. *The Journal of Physical Chemistry Letters* **2020**, *11*, 3089–3094.

(16) Guo, H.; Poths, P.; Sautet, P.; Alexandrova, A. N. Oxidation Dynamics of Supported Catalytic Cu Clusters: Coupling to Fluxionality. *ACS Catalysis* **2021**, *12*, 818–827.

(17) Peters, B. Simple Model and Spectral Analysis for a Fluxional Catalyst: Intermediate Abundances, Pathway Fluxes, Rates, and Transients. *ACS Catalysis* **2022**, *12*, 8038–8047.

(18) Yan, G.; Vlachos, D. G. Unraveling Multiscale Kinetics over Subnanometer Cluster Catalysts: H_2 Desorption from $Pt_3(-H)_2/\gamma$-$Al_2O_3(110)$. *ACS Catalysis* **2023**, 10602–10614.

(19) Xing, X.; Li, X.; Yoon, B.; Landman, U.; Parks, J. H. Dynamic fluxionality and enhanced CO adsorption in the presence of coadsorbed H2O on free gold cluster cations. *International Journal of Mass Spectrometry* **2015**, *377*, 393–402.

(20) Zhai, H.; Alexandrova, A. N. Ensemble-Average Representation of Pt Clusters in Conditions of Catalysis Accessed through GPU Accelerated Deep Neural Network Fitting Global Optimization. *Journal of Chemical Theory and Computation* **2016**, *12*, 6213–6226.

(21) Kresse, G.; Furthmüller, J. Efficient iterative schemes foriab initio/itotal-energy calculations using a plane-wave basis set. *Physical Review B* **1996**, *54*, 11169–11186.

(22) Perdew, J. P.; Burke, K.; Ernzerhof, M. Generalized Gradient Approximation Made Simple. *Physical Review Letters* **1996**, *77*, 3865–3868.

(23) Blöchl, P. E. Projector augmented-wave method. *Physical Review B* **1994**, *50*, 17953–17979.

(24) Steinmann, S. N.; Corminboeuf, C. A generalized-gradient approximation exchange hole model for dispersion coefficients. *The Journal of Chemical Physics* **2011**, *134*.

(25) Gautier, S.; Steinmann, S. N.; Michel, C.; Fleurat-Lessard, P.; Sautet, P. Molecular adsorption at Pt(111). How accurate are DFT functionals? *Physical Chemistry Chemical Physics* **2015**, *17*, 28921–28930.

(26) Zhai, H.; Sautet, P.; Alexandrova, A. N. Global Optimization of Adsorbate Covered Supported Cluster Catalysts: The Case of $Pt_7H_{10}(CH_3)$ on Al_2O_3. *ChemCatChem* **2019**, *12*, 762–770.

(27) Henkelman, G.; Uberuaga, B. P.; Jónsson, H. A climbing image nudged elastic band method for finding saddle points and minimum energy paths. *The Journal of Chemical Physics* **2000**, *113*, 9901–9904.

(28) Sheppard, D.; Xiao, P.; Chemelewski, W.; Johnson, D. D.; Henkelman, G. A generalized solid-state nudged elastic band method. *The Journal of Chemical Physics* **2012**, *136*.

(29) Loffreda, D.; Delbecq, F.; Simon, D.; Sautet, P. Breaking the NO bond on Rh, Pd, and Pd3Mn alloy (100) surfaces: A quantum chemical comparison of reaction paths. *The Journal of Chemical Physics* **2001**, *115*, 8101–8111.

(30) Voter, A. F. *Radiation Effects in Solids*; Springer Netherlands, pp 1–23.

(31) Zandkarimi, B.; Sun, G.; Halder, A.; Seifert, S.; Vajda, S.; Sautet, P.; Alexandrova, A. N. Interpreting the Operando XANES of Surface-Supported Subnanometer Clusters: When Fluxionality, Oxidation State, and Size Effect Fight. *The Journal of Physical Chemistry C* **2020**, *124*, 10057–10066.

(32) Poths, P.; Sun, G.; Sautet, P.; Alexandrova, A. N. Interpreting the *Operando* X-ray Absorption Near-Edge Structure of Supported Cu and CuPd Clusters in Conditions of Oxidative Dehydrogenation of Propane: Dynamic Changes in Composition and Size. *The Journal of Physical Chemistry C* **2022**, *126*, 1972–1981.